Polymer Degradation and Stability 126 (2016) 134–143

Contents lists available at ScienceDirect

Polymer Degradation and Stability

journal homepage: www.elsevier.com/locate/polydegstab

Influence of surface modified nano silica on alkyd binder before and after accelerated weathering

Miroslav Nikolic [a, *], Hiep Dinh Nguyen [b], Anders Egede Daugaard [b], David Löf [c], Kell Mortensen [d], Søren Barsberg [a], Anand Ramesh Sanadi [a, **]

[a] Department of Geosciences and Natural Resource Management, IGN, University of Copenhagen, Rolighedsvej 23, DK-1958 Frederiksberg C, Denmark
[b] Department of Chemical and Biochemical Engineering, Technical University of Denmark, Søltofts Plads, Bygning 227, DK-2800 Kgs., Lyngby, Denmark
[c] PPG Architectural Coatings EMEA, Dyrup A/S, Gladsaxevej 300, DK-2800 Søborg, Denmark
[d] Niels Bohr Institute, X-ray and Neutron Science, University of Copenhagen, Universitetsparken 5, DK-2100 København Ø, Denmark

ARTICLE INFO

Article history:
Received 22 October 2015
Received in revised form
18 January 2016
Accepted 8 February 2016
Available online 9 February 2016

Keywords:
Alkyd
Exterior wood coatings
Nanocomposites
Surface modification
Nano silica
Accelerated weathering

ABSTRACT

Introduction of nano fillers in exterior wood coatings is not straight forward. Influence on aging of polymer binder needs to be taken into account along with possible benefits that nano fillers can provide immediately after application. This study shows the influence of two differently modified hydrophobic nano silica on an alkyd binder for exterior wood coatings. One month after application, the highest strength and energy required to break the films was obtained with addition of 3% disilazane modified silica. Changes in tensile properties were accompanied with a small increase in glass transition temperature. However, the highest stability upon accelerated weathering, measured by ATR-IR and DMA, was for nano composites with the highest amount of nano filler. The reasons for the observed changes are discussed together with the appearance of a feature that is possibly a secondary relaxation of alkyd polymer.

1. Introduction

Use of nanotechnology is increasing in the wood coating industry. Reinforcement of interior wood coatings presents a clear benefit for parquet lacquers and furniture coatings where mechanical resilience is a very important parameter. In exterior wood coatings nano fillers are presently predominantly used to improve UV protection; although superhydrophobic, self-cleaning coatings or nano based preservatives are likely to be important in the future [1].

Addition of nanofillers in exterior coatings usually impacts mechanical properties. Mechanical properties are typically considered of secondary importance for exterior wood coatings, but their improvements will of course always be viewed as favorable. With a slow change towards biobased materials in the coating industry, the limiting constraint can be that they often have weaker mechanical properties compared to conventional materials [2,3]. Manipulation of these properties can become more important in the future. When hard inorganic nano particles are added into a polymer matrix an increase in stiffness is often seen. However, of much higher importance is the flexibility and toughness of exterior wood coating as it needs to follow the movement of wood without cracking for a prolonged period of several years [4]. Dimensional changes of wood due to absorption/desorption of water are a cause of constant stress on the wood coating and could lead to fatigue failure. The difference in thermal expansion coefficient of wood and coating is another cause of stress on the protective coating [5–8]. As polymer glass transition temperature (T_g) affects the flexibility a lot, influence of coating constituents on polymer T_g and on the T_g stability over time will be of utmost importance.

Due to the large surface area of the nanofillers increased stiffness and restrictions in polymer chain mobility should occur with the addition of nanofiller, and polymer T_g usually increases to a certain extent. However, when tests were performed after

* Corresponding author.
** Corresponding author.
E-mail addresses: mirn@ign.ku.dk (M. Nikolic), anrs@ign.ku.dk (A.R. Sanadi).

http://dx.doi.org/10.1016/j.polymdegradstab.2016.02.006
0141-3910/

weathering on exterior coatings, it was seen that nano particles can have different effect on T_g. Both an increased or decreased stability of T_g over time, compared to the nano filler free controls, was seen [9–11]. This means that the polymer-particle interface and the interactions between the polymer and filler have an influence on the T_g. The stability of T_g over time can potentially also be affected by the presence of surface active compounds which are often used as dispersing aids for preparation of nano composites.

To the best of our knowledge there are no studies from this perspective with the use of nano silica in wood coatings. Nano silica was shown to improve mechanical properties of interior wood coatings like abrasion and scratch resistance [12,13] or stiffness and tensile strength [14,15]. A well-known effect of nano silica as a toughening agent for brittle polymers like epoxides [16] can become important with stiffening of exterior wood coating over time. A long oil alkyd was chosen as a binder in this study. The basic structure of an alkyd polymer is given in Fig. 1. Alkyds have for a long time been one of the first choices as binders in exterior wood coatings due to their high flexibility, very good penetration into the wood and pigment wetting [17]. Even solvent based alkyd coatings still have a large market share in wood coating industry [18].

In the current investigation, silica particles with different surface chemistries were investigated to determine the effect of a hydrophobic surface coating as well as a reactive particle surface of intermediate polarity. A hydrophobic, hexamethyl disilazane (HMDS) treated nano silica that should have good compatibility with alkyd polymer was used. In recent time and probably even more in the future, water based coatings are increasingly represented, especially in the do-it-yourself part of the market that has a large share in exterior wood coatings. For this reason, it is important to know if the nano filler behaves in the same manner in both solvent and water borne formulations. Tests with low amount of nano filler, that typically provides best results in respect to nanocomposites, were performed in both solvent and water borne formulations. We have also chemically modified hydrophilic nano silica with tall oil fatty acids. This modification increases the compatibility and interactions with the alkyd polymer, and also allows us to study the effect of crosslinking the nano filler with the polymer matrix. Results from one month after coating application and after accelerated weathering are reported and discussed.

2. Materials and methods

2.1. Chemical compounds

A 100% solid long oil alkyd polymer (60% oil length, acid number = 7) typically used for exterior wood coatings was obtained from PPG Architectural Coatings EMEA, Dyrup A/S together with siccatives (for solvent and water borne coatings), white spirit, industrial emulsifiers, defoamer and tall oil fatty acids (TOFA). The majority of the TOFA sample comprised of the 9,12-octadecadienoic acid (C18:2) and 9-octadecenoic acid (C18:1), which accounted for approximately 48 wt% and 33 wt% of the whole mixture, respectively. All other chemicals were at analytical grade and were used as bought from Sigma Aldrich.

2.2. Nano silica filler

Hexamethyl disilazane treated nano silica (further abbreviated as S1) in powder form (20 nm particle size) was used as obtained from Fluorochem Ltd. 7 nm glycidoxypropyl modified colloidal nano silica (S2) commercially known as Bindzil CC 301 was obtained from PPG Architectural Coatings EMEA, Dyrup A/S and this silica was further modified with TOFA. Model structures of different silica used are shown in Fig. 2.

2.3. Nano silica modification with TOFA

2.3.1. Preparation of TOFAoyl chloride

TOFA (71.21 g, 0.25 mol) was transferred into a one necked flask and dried using an excess amount of dry toluene and a rotary evaporator. A magnetic bar is then added to the reaction mass and the temperature was reduced to 0 °C using an ice and salt bath. Oxalyl chloride (141.37 g, 1.11 mol) was then transferred dropwise into the reaction mass followed by 10 drops of dimethylformamide (DMF). A condenser was fitted onto the system and connected to a nitrogen supply. Reaction mass was then heated to 80 °C for 3.5 h, whereafter the product was isolated by evaporation of the excess reagents. The product was used without further purification.

2.3.2. TOFA grafted silica

The S2 silica to be modified was provided as a dispersion in water, and subsequent lyophilization was carried out to yield a dried sample at mild conditions. The dried S2 (29.28 g) and a magnetic bar was added to a one necked flask followed by adding of dichloromethane. In a separate Erlenmeyer flask 4-dimethylaminopyridine (DMAP, 3.28 g, 0.03 mol) was dissolved with a small amount of dichloromethane and then mixed with triethylamine (52.93 g, 0.52 mol) to make a clear solution. This solution was then added to the flask and the reaction mass was cooled to below 0 °C using an ice and salt bath. TOFAoyl chloride (76.16 g, 0.25 mol) was diluted with dichloromethane and then added drop wise to the reaction mass. The reaction was then carried out at room temperature under nitrogen overnight. The reaction was stopped and diluted with dichloromethane and the resulting dispersion was filtered and dried *in vacuo* at room temperature, to yield the TOFA modified silica (mS2) (Fig. 2b).

2.4. Preparation of the coatings

Nano silica was added into the alkyd polymer and dispersed with the use of SpeedMixer DAC 150.1 FVZ-K. Mixing time was 1 min at 1000 rpm and then 3min at 3000 rpm for 3 wt% of nano silica (S1 and mS2). For 8 wt% of S1, the mixing time was 1 min at

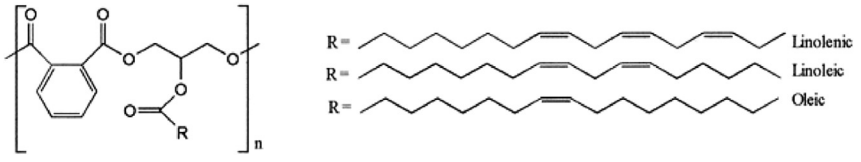

Fig. 1. Alkyd structure (Reproduced with permission from Ref. [19]).

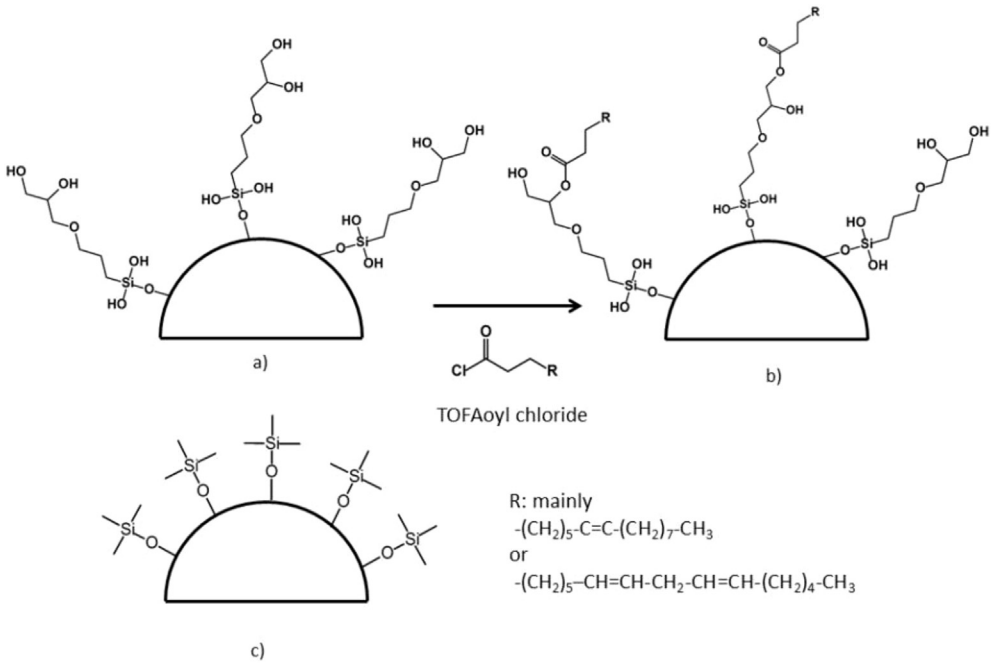

Fig. 2. Model structures of different silica fillers: a) glycidoxypropyl modified nano silica (S2); b) TOFA modified nano silica (mS2); c) hexamethyl disilazane treated nano silica (S1).

1000 rpm and 2 × 3min at 3000 rpm.

2.4.1. Preparation of solvent based formulations

For the solvent based formulations, pure alkyd or alkyd-silica mixture was diluted with white spirit and siccatives were stirred in on Ultraturrax mixer. No further additives were added.

2.4.2. Preparation of water based formulations

Pure alkyd and alkyd with 3% S1 were emulsified in water at 65 ± 5 °C and low shear mixing at 200 rpm. The procedure is briefly described as following. Preheated non-ionic and anionic surfactants were first added into 50 g of polymer (or into polymer and 3% S1 mixture) and mixed for 15min. The alkyd was then neutralized with the use of 45% solution of potassium hydroxide. Water was slowly added for a duration of 2 h with an automated syringe pump to final 50 wt% emulsion solid content.

Defoamer and siccative were finally added to the emulsion and stirred in using the Ultraturrax mixer. No other additives were used.

All the coatings films that are studied and compared in this article are described in Table 1.

2.5. Characterization

1D and 2D Nuclear Magnetic Resonance spectra were measured using a Bruker Avance [300 MHz (^{1}H) and 75 MHz (^{13}C)] using $CDCl_3$ as the solvent. Thermal Gravimetric Analysis (TGA) data was recorded on a TA Q500 from TA Instruments. Samples were heated from room temperature to 700 °C at a rate of 10 °C/min under nitrogen. The average emulsion droplet size was determined by dynamic light scattering performed on a NanoBrook Omni Particle Size Analyzer from Brookhaven Instruments Corporation with 640 nm light wavelength.

Tensile tests were carried out following the ASTM D2370 standard and using a Shimadzu testing machine (AGS-X, 20N load cell) with the crosshead speed of 15 mm/min. Gauge length was 25 mm with the sample width of 6.5 mm and thickness 0.050 ± 0.010 mm. Dynamic mechanical analysis (DMA) was performed in tension mode on TA instruments Q800 analyzer. The DMA analysis is well known method employed in order to study the relationship between structure and properties of the material. Through the evaluation of storage and loss modulus and tan delta information can be obtained about glass transition

Table 1
Summary and description of all the samples that are compared in this study.

Solvent based coatings that are compared:	
SB alkyd	films obtained from pure alkyd binder
3% S1 in SB alkyd	films obtained from alkyd binder that contains 3 wt% of HMDS modified nano silica
8% S1 in SB alkyd	films obtained from alkyd binder that contains 8 wt% of HMDS modified nano silica
3% mS2 in SB alkyd	films obtained from alkyd binder that contains 3 wt% of TOFA modified S2 nano silica
Water based coatings that are compared:	
WB alkyd	films obtained from alkyd emulsion
3% S1 in WB alkyd	films obtained from alkyd emulsion that contain 3 wt% of HMDS modified nano silica

temperature, secondary transitions, crosslinking, aging, effect of additives and other [20]. In nano composites the DMA is often used to study the influence of nano particles on polymer viscoelastic properties. However if the tests are also performed after weathering the change of T_g can be determined. The T_g stability upon weathering is now commonly used to characterize material aging [21]. For the pure polymer, besides the T_g stability, values of the storage modulus in the rubbery plateau can be related to the crosslinking density, which also changes upon weathering. Before accelerated weathering, samples were measured from −40 to 80 °C (2 °C/min, 1Hz, strain rate 0.4%). Gauge length was 10 mm, sample width 3.0 mm and thickness 0.050 ± 0.010 mm. After accelerated weathering, samples were measured from 20 to 160 °C keeping the rest of the settings unchanged. Attenuated total reflectance IR (ATR-IR) spectroscopy was performed by a Thermo Nicolet 6700 FT-IR spectrometer equipped with a Golden Gate (diamond) ATR accessory and DTGS (KBr) detector. It is one of the advantages of ATR-FTIR spectroscopy that there is no sample preparation; it is well known that the sample must simply be brought into close contact with the ATR crystal surface after which the spectrum can be acquired. All spectra were obtained in the 4000–400 cm^{-1} range by 100 scans at 4 cm^{-1} resolution. Atmospheric suppression and advanced ATR correction (software options: 45° angle of incidence, number of bounces equal to 1 and sample refractive index was taken as 1.60) were performed on all spectra before straight line subtraction (points taken at 1840 and 3800 cm^{-1}) and normalization with the absorption maximum of the CH_2 bending vibrations at 1460 cm^{-1}.

Accelerated weathering was carried out in a QUV Accelerated Weather Tester (09-15477-77/spray) following conditions described in EN 927-6. After initial condensation step at 45 °C, cycles of UV irradiation (340 nm, 60 °C and 2.5h) and water spraying (0.5 h) were performed for a total of 200 h. The reason for this short time period is because no UV absorbers were used and significant changes in polymer matrix already occurred. In a pre-test of pure alkyd that was exposed to these conditions the film started to fail by flaking after around 300 h of exposure.

The prepared coatings were applied with a manually operated draw down applicator to a Teflon board to obtain free films after curing. The films were carefully removed and cut to appropriate sizes for testing. Tests were performed one month after application. For accelerated weathering tests, the mixtures were applied on metal plates (15 cm × 8 cm) previously covered by Teflon tape and left to cure for one month before placing them in the weathering chamber.

3. Results and discussion

mS2 particles were obtained through a two-step process, where initially the acid chloride of TOFA was prepared from commercially available TOFA using oxalyl chloride. Full conversion of the acid was confirmed using ^1H and ^{13}C NMR. The signals from the methylene groups next to the carbonyl group shifted from 2.35 to 2.88 ppm in the ^1H NMR spectra (Appendix Figures A.1). A characteristic shift of the C=O signal from 180.3 to 174.0 ppm in the ^{13}C NMR spectra (Appendix Figures A.2) was also seen.

The derivatization of the particles was confirmed by thermogravimetric analysis (TGA), for both the precursor (lyophilized S2) as well as the mS2 particles (Appendix Figures A.3). The decomposition process of the original silica can be divided into two parts, from approximately 75°C–250 °C, and from 250°C to 650 °C. After modification an increase of the weight loss in the higher temperature regime was observed. The difference between the weight loss in the modified particles and the pristine starting material was assigned to the TOFA modification, which results in a derivatization with fatty acid of 5.17 wt % (Appendix Table A.1). Due to the relatively low degree of modification, particles with an intermediate polarity (both hydrophilic and hydrophobic parts) are obtained. TOFA derivatives on the mS2 particle surface additionally enable participation in the curing of the alkyd. Also, from the TGA curves it can be seen that the mS2 shows a higher number of degradation steps than S2. This is possibly because acylation of different types of hydroxyl groups in the pristine silica (S2) with TOFA may result in the modified material (mS2) with sections bearing different level of thermal-stability.

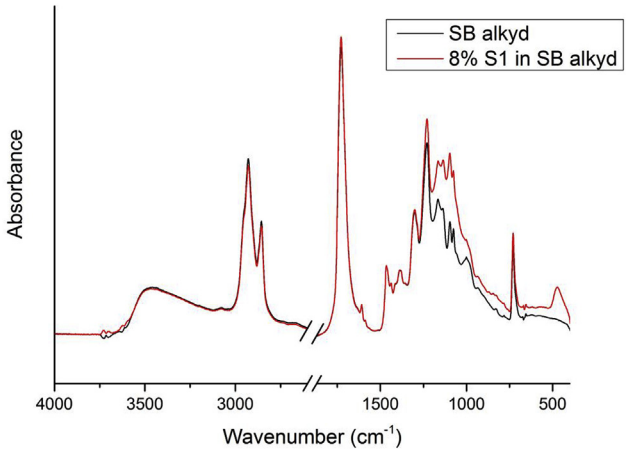

Fig. 3. Changes in the pure alkyd (black line) spectrum after the addition of nano silica (red line). (For interpretation of the references to colour in this figure legend, the reader is referred to the web version of this article.)

In solvent borne (SB) formulation, it was noticed that mS2 silica started to sediment during storage while the S1 silica was stable. Sedimentation of mS2 probably occurred because some of the Si–OH polar groups on TOFA modified silica were still exposed leading to agglomeration over time in this environment. Further stabilization and dispersion of this silica would probably require choosing an appropriate surfactant (or surfactant combination) [22]. However, having additional surfactants could also affect the (long term) behavior of the entire coating compared to the other systems [23,24]. Since the primary aim was to study the influence of nano silica on the alkyd binder it was decided not to add additional dispersing aids even though micron size clusters are most likely present in this silica-alkyd combination. Dispersion of the lyophilized S2 in the pure alkyd was also attempted but the agglomerates of filler particles were clearly visible with the naked eye indicating that proper dispersion of such hydrophilic filler is probably not possible in the pure alkyd polymer. Due to this issue no further tests were performed with the pristine S2.

For water borne (WB) formulations the pH was 8.2–8.3 and mean droplet size, determined with the use of dynamic light scattering, was 187 ± 3 nm for both pure alkyd and with 3%S1. This means that the silica is probably contained within the alkyd emulsion droplet and also indicates that the silica is possibly well dispersed and is within the nano range.

Table 2
IR band assignments for the alkyd coating [26–31].

Wavenumber (cm^{-1})	Assignment
728	aromatic C–H out of plane bending or CH_2 rocking
1070 - 1300	C–O, C–O–C, CH_2–O stretching
1398	CH bending
1460	CH_2 bending
1589 and 1608	C=C aromatic ring stretching
1632	C=C aliphatic stretching
1721	C=O stretching
2854	CH_2 asymetric stretching
2925	CH_2 symetric stretching
3460	O–H stretching

3.1. Air cured samples for one month

3.1.1. Attenuated total reflectance IR spectroscopy

Fig. 3 shows ATR-FTIR spectra of a pure alkyd and alkyd with 8% S1 nano silica. The most significant bands for the alkyd polymer are tentatively assigned in Table 2. With the addition of nano silica a characteristic new peak centered at 462 cm^{-1} was found and it can be assigned to Si-0-Si bending. Significant changes in intensity and shape of spectra between 1000 and 1200 cm^{-1} were also seen due to contribution of Si–O–Si asymmetric stretching vibrations [25]. No other changes in intensity or position of peaks due to addition of nano silica were found. With 3% of S1 and with mS2 silica, spectra were qualitatively the same as the one in Fig. 3.

3.1.2. Dynamic mechanical analysis

Results of DMA tests are shown in Table 3. Storage modulus is presented at typical temperatures to which exterior coatings are exposed. Glass transition temperature (T_g) was assigned following ASTM E1640 – 13 standard to storage modulus onset point but Table 3 also contains tan delta values. Dependence of average storage modulus on temperature for all the samples is shown in Appendix Figures A.4. It is observed that the water based alkyd had around 15 °C lower T_g compared to the pure polymer film obtained from a solution in organic solvent. This sort of film plasticization can be related to the presence of small surface active emulsifiers and also possibly the neutralizing agent. This plasticization will in general reduce alkyd mechanical properties; however, it will also enable the film formation without the use of additional volatile organic compounds (VOC) as coalescing aids.

Addition of nano silica had a small influence on T_g. Highest T_g was measured with 8% of nano filler and the increase was only about 4 °C. Among the samples, the highest storage modulus below the T_g was with mS2 silica which is probably due to co-valent bonding of these particles with the alkyd polymer. Storage modulus did increase significantly with the incorporation of nano silica (up to 80%) but above the T_g. The large increase above T_g can be explained by the constraint on the polymer in the proximity of nano particles with high surface area. Volume next to the nano particles can have properties that are different compared to the rest of the polymer. In this interfacial area, due to interactions with the nano filler, there is reduced movement of polymer chain segments and an increased stiffness probably leading to observed changes in properties. The local changes in polymer relaxation in the proximity of nano fillers are further supported by the increase in width of loss modulus peak [32] (Appendix Figures A.5.).

3.1.3. Tensile properties

Table 4 summarizes the tensile properties of all the films. As expected from DMA results, water based systems had, in general, lower mechanical properties at room temperature due to the reduced T_g. Introduction of 3 wt% S1 silica increased the modulus

Table 3
Storage modulus at different temperatures together with glass transition temperature for all the solvent borne (SB) and water borne (WB) coatings.

Sample	T_g - E′ onset point (°C)	tan delta (°C)	E′ (MPa)		
			0 (°C)	20 (°C)	40 (°C)
Solvent borne systems					
SB alkyd	19.0	43.7	1502	740	46.1
3% S1 in SB alkyd	19.6	46.5	1530	800	70.0
8% S1 in SB alkyd	23.6	47.1	1599	909	82.7
3% mS2 in SB alkyd	18.7	46.2	1674	830	77.4
Water borne systems					
WB alkyd	5.4	30.8	693	95	5.7
3% S1 in WB alkyd	6.0	31.3	827	114	6.3

Table 4
Tensile properties of pure alkyd and different nano composites.

Sample	Elastic modulus (MPa)	Tensile strength (MPa)	Elongation at break (%)	Energy to break ($J \cdot 10^3$)
Solvent borne systems				
SB alkyd	91.7 ± 17.9	12.2 ± 1.4	92.8 ± 9.6	54.0 ± 5.9
3% S1 in SB alkyd	105.0 ± 17.1	12.8 ± 1.6	92.2 ± 7.6	73.5 ± 11.4
8% S1 in SB alkyd	128.2 ± 23.0	11.2 ± 0.7	73.7 ± 5.9	43.7 ± 4.3
3% mS2 in SB alkyd	104.2 ± 12.9	7.5 ± 0.3	51.2 ± 3.6	27.1 ± 2.5
Water borne systems				
WB alkyd	3.5 ± 0.2	3.6 ± 0.6	90.9 ± 9.0	12.0 ± 3.0
3% S1 in WB alkyd	4.2 ± 0.2	4.0 ± 0.6	94.5 ± 10.4	16.3 ± 4.9

without reducing the elongation at break. Also, energy needed to break the films strongly increased at this loading level by 35%. Enhancement of mechanical properties in this manner with spherical nano fillers requires high compatibility between nano filler and polymer matrix [33]. It appears that the compatibility was achieved and that polymer-filler interfacial interactions are allowing the stress transfer to the filler during straining leading to higher energy needed to break the material. It is important to note that the way tensile properties changed with the addition of 3% of S1 was the same in solvent borne and water borne formulations. This means that the hydrophobic filler was well protected from the water environment, possibly within the alkyd droplet. During and after evaporation of water, agglomeration of this nano filler should not be different compared to solvent borne formulation as the polymer-filler interactions are the same.

Increasing the loading of this silica to 8% further improved the modulus but the other tensile properties were worsened. As the amount of nano filler increased, the dispersion was probably no longer as good and some agglomerates might be present leading to certain level of stress concentrations in the film. Addition of mS2 silica, already at 3%, showed high decrease in all the properties except in relation to elastic modulus that increased. Due to high agglomeration in some areas these films behave more like composites with uneven microfillers instead of well dispersed nanofillers. Previous studies on nano silica covalently bonded to the organic polymer show possibilities in improving multiple properties like strength, modulus, scratch and abrasion resistance [12,34,35] at the same time. In order to further exploit possible crosslinking of this nano silica into the alkyd polymer (and not just to increase the stiffness) better dispersion would be necessary.

3.2. Samples tested after accelerated weathering

3.2.1. Attenuated total reflectance IR spectroscopy

Significant and very complex changes occur in the alkyd matrix during the aging of the coating, but they have been well studied in the past. One of the processes is the ongoing autoxidation that is responsible for continuous increase in cross linking density. With the new cross links, an increasing amount of ether bonds and decrease of unsaturation is seen [36]. Multiple secondary oxidation reactions are also occurring leading to different carbonyl moieties

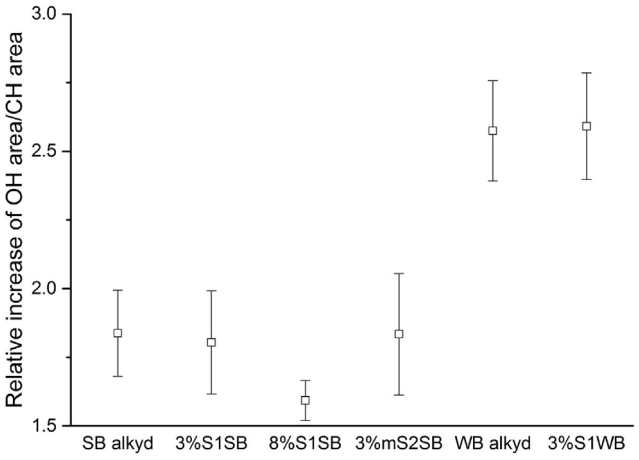

Fig. 5. Relative increase of hydroxyl band area after accelerated weathering for pure alkyd coatings and all the nanocomposites.

that finally oxidize to carboxylic acids. Beta scission is one of these and leads to cleavage of part of the aliphatic chain [37]. In the outdoor conditions hydrolysis of the polyester is also present increasing the number of hydroxyl species [28,38]. Carboxylic acids formed during the oxidation can also catalyze the hydrolysis accelerating the alkyd degradation. As can be seen, several pathways can interact.

IR spectroscopy after the accelerated weathering detects the sum of all these changes and the average spectra of pure alkyd before and after the QUV are shown in Fig. 4. Hydrolysis and beta scission appear dominant in these conditions. After the accelerated weathering a decrease in carbonyl stretching intensity is accompanied with appearance of a new peak around 1570 cm^{-1}. This new peak is related to COO^- anions asymmetric vibrations of carboxylic acid salts [39,40] formed during the aging of the coating. A marked decrease in CH_2 stretching (2854 and 2925 cm^{-1}) was also detected along with an increase of the hydroxyl peak. The center of the hydroxyl peak has also shifted to

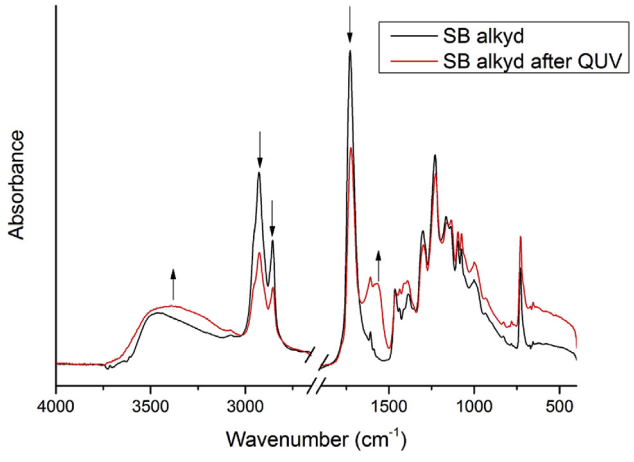

Fig. 4. Average ATR-FTIR spectra of solvent based alkyd coating before and after accelerated weathering (most significant changes are marked with arrows).

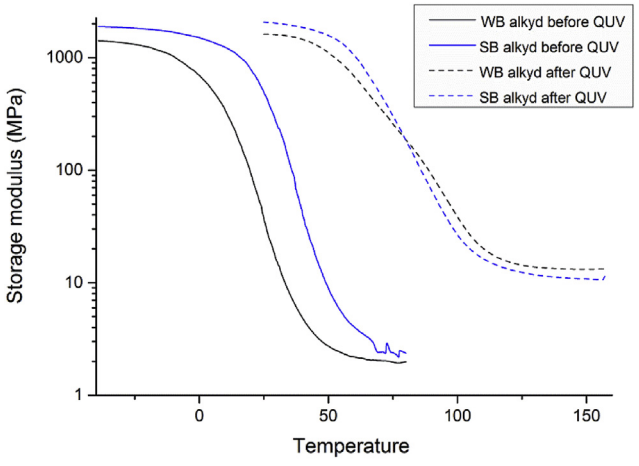

Fig. 6. Storage modulus for water based alkyd (WB, black) and solvent based alkyd (SB, blue) before (full line) and after (dash line) accelerated weathering. (For interpretation of the references to colour in this figure legend, the reader is referred to the web version of this article.)

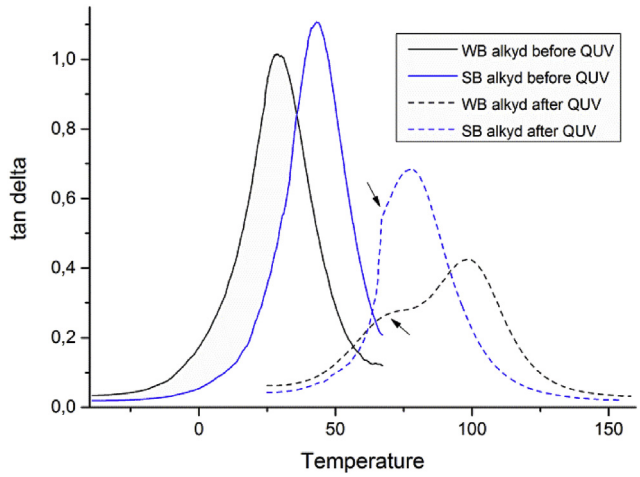

Fig. 7. Tan delta for water based alkyd (black) and solvent based alkyd (blue) before (full line) and after (dash line) accelerated weathering. (For interpretation of the references to colour in this figure legend, the reader is referred to the web version of this article.)

smaller wavenumbers signifying stronger and/or more extended hydrogen bonding.

In order to determine the effect of nano silica a semi-quantitative study was performed by looking at the change, due to exposure to QUV, of OH peak area (3100–3630 cm^{-1}) normalized by CH_2 stretching area (2700–3000 cm^{-1}) [41]. Larger changes after the same amount of time signify faster degradation. Water based alkyds degraded faster than solvent based ones (Fig. 5), and these are in general considered more porous. Furthermore, the emulsifiers can leach out to the film surface over time further increasing water sensitivity. All this leaves the film more exposed to attack by water. With hydrolysis being one of the main degradation routes, it is not a surprise that the water based coating was degrading faster. One of the ways to tackle these problems would be to use surfactants that polymerize with the latex particles [42] and remain bound in the film. These results confirm the well-known fact how much care should be given to the best possible film formation with water based coatings in order to achieve appropriate protection. Addition of 3% nano filler had little influence on the aging of the alkyd and results are practically the same as for the pure polymer. However, adding 8% of disilazane modified silica slowed down the increase of hydroxyl band. Higher amount of silica nano filler, although possibly agglomerated to a certain extent, probably provided an increased protection from water by filling the cavities in the films as often seen in different silica based nanocomposites [43–45].

3.2.2. Dynamic mechanical analysis

Most of the reactions during aging lead to increased stiffness and embrittlement of the alkyd. Over time T_g will increase, and how stable the film is in respect of T_g is of great importance for exterior wood coatings. Under the QUV conditions a substantial change of T_g occurred. Figs. 6 and 7 display storage modulus and tan delta values for solvent borne and water borne alkyd before and after accelerated weathering. The storage modulus in the rubbery plateau increased multiple times upon aging. For the pure thermosetting polymer, the rubbery plateau is related to the crosslinking density [46] so this change was expected with the ongoing autoxidation of the alkyd. In the glassy region, storage modulus is practically the same as before the weathering. The T_g of the water based alkyd increased much faster compared to the solvent borne counterpart. The plasticization of the water borne alkyd is not permanent and it will disappear with the leaching out of the surfactants, and eventually the two systems should have practically the same T_g. However, further increase of T_g for water borne alkyd is because of faster aging and degradation as seen also from the FTIR results. Further support of this claim is the much higher decrease of tan delta intensity for water based alkyd. This means that the water based alkyd lost much more of its capability to dissipate energy and relax upon loading.

Another feature that became apparent upon aging is what we believe to be a secondary relaxation around 20–30 °C below tan delta maximum (Fig. 7). This was not seen before QUV probably because it was hidden by the high intensity of the main relaxation peak. It is also much clearer in the WB alkyd where the tan delta intensity is lower. The secondary relaxations of alkyds are practically not studied. We have recently reported one relaxation of the non-aged alkyd [47] around 100 °C below tan delta maximum which could belong to the rotation of the side groups.

A relaxation positioned this close to the T_g can be related to a motion of few carbon atoms around the main chain and it is often used to describe the high toughness of certain polymer groups [48]. Other possibilities also exist to explain the origin of this phenomenon. Due to degradation an overall wider distribution in relaxation of the polymer matrix is now possible, and that may lead to tan delta peak separation. Also, degradation is larger in the surface part of the film compared to the part closer to the substrate, and it may be possible to see a separated transition even though the film was applied as a single layer. Further studies in order to confirm this relaxation can prove to be important for better understanding of alkyd coatings.

With the increase in the crosslink density and the T_g, alkyds eventually start cracking as they are no longer capable of following

Table 5
Influence of accelerated weathering on viscoelastic properties of alkyd coating and nanocomposites (* is explained in the text).

Sample	E′ onset point (°C)		tan δ (°C)		tan δ intensity	
	Before QUV	After QUV	Before QUV	After QUV	Before QUV	After QUV
Solvent borne systems						
SB alkyd	19.0	59.2	43.7	87.2	1.11	0.68
3% S1 in SB alkyd	19.6	50.0*	46.5	75.1*	0.99	0.65*
8% S1 in SB alkyd	23.6	53.5	47.1	86.5	1.03	0.60
3% mS2 in SB alkyd	18.7	59.7	46.2	92.7	0.99	0.52
Water borne systems						
WB alkyd	5.4	57.5	30.8	96.5	1.03	0.43
3% S1 in WB alkyd	6.0	57.9	31.3	98.6	1.07	0.35

the movement of wood and distributing stress. It is possible that due to this relaxation alkyds can remain without cracks well below their T_g under low strains (below 15% [49]) induced by the dimensional changes of wood substrate.

In this study, it was also essential to know the effect of nano silica on the T_g after QUV. Some studies on acrylic based coatings have shown that with the introduction of nano particles there is a possibility that T_g increases faster than for the pure polymer leading to earlier cracking of the film [11]. This was not the case in our study where the fillers in general have good compatibility with the polymer matrix (Table 5). It needs to be said that 3% S1 in SB alkyd films used for QUV had a 30 μm higher thickness compared to the other samples. As the thicker samples will be less degraded after same amount of time and the film thickness itself can influence the T_g [38] the DMA results of that nano composite are considered as unreliable. All other samples tested before or after weathering had thickness within ±5 μm compared to the pure alkyd coatings. The influence of nano silicas on viscoelastic properties is to a big part the same as before the QUV. However, the overall lowest measured T_g (53.5 °C) is with 8%S1 in SB alkyd which corroborates well with the FTIR data. It also signifies that the dominant factor on T_g stability is the influence on polymer aging as composites with 8%S1 in SB alkyd had the highest T_g one month after application.

The decrease of tan delta intensity with the addition of nano fillers was present as typically when nano fillers are used. The decrease was overall small, again probably due to good compatibility and low restriction of relaxation, and it remained such after accelerated weathering. Highest decrease of tan delta intensity was with 3%S2 either because of bad dispersion or due to the actual crosslinking of this silica in the polymer.

4. Conclusions

Reinforcement of exterior wood coatings needs to be performed with great care as large increase in T_g can potentially have a negative effect on long term coating flexibility. This study shows that with good compatibility between nano silica and the polymer matrix reinforcement is not detrimental for long term performance, even for outdoor wood coatings. When tested one month after application, best results were obtained with adding 3% of disilazane modified nano silica. An increase in stiffness and energy needed to break was accompanied with a small influence on T_g and the same trends were seen in both solvent borne and water borne formulations. However, FTIR and DMA tests after accelerated weathering showed that higher amount of 8% nano silica was actually capable of slowing down the alkyd degradation to a certain extent probably by providing increased protection from water and hydrolysis. Based on these results, nano fillers with high aspect ratios could provide even further benefits and should be tested in the future.

Chemical modification of nano silica with tall oil fatty acid showed potential to increase the modulus of elasticity. This modification is interesting as it may allow the nano filler to covalently bind into the alkyd film. To further exploit this effect an improved dispersion with the use of surface active compounds will be necessary. Surfactants were seen in the past to greatly influence film behavior, and special care should be taken in order to make the right choice for polymer-surfactant-filler combinations.

Another feature that was found after accelerated weathering is a possible secondary relaxation of alkyd polymer; this type of relaxation can have an influence on polymer toughness and further research in this phenomenon is needed for polymers used in exterior wood coatings.

Acknowledgement

We would like to acknowledge the Innovation Fund Denmark, previously known as Danish High Technology Foundation, for the financial support through “Superior Bio based Coating System for Exterior Wood Applications” project, file number 056-2011-3. We would also like to acknowledge Nina Axelsen and Jannie Jensen from PPG Architectural Coatings EMEA, Dyrup A/S for help regarding accelerated weathering tests.

Appendix

NMR Analytical data:

δ_H (300 MHz, $CDCl_3$): 5.45–5.28 (m, =C<u>H</u>–), 2.77 (t, J = 5.7 Hz, =HC–C<u>H</u>$_2$–CH =), 2.2.35 (t, J = 7.5 Hz, –C<u>H</u>$_2$–COO–), 2.18–1.98 (m, –C<u>H</u>$_2$–CH=CH), 1.75–1.58 (m, –C<u>H</u>$_2$–), 1.31–1.27 (m, –C<u>H</u>$_2$–), 0.91–0.86 (m, –C<u>H</u>$_3$).

δ_C (75 MHz, $CDCl_3$): 180.3 (–COOH), 130.4–128.0 (sp^2 = <u>C</u>H–), 34.2, 33.6 (–<u>C</u>H$_2$–COOH), 32.1, 31.7, 29.9–29.2, 22.8, 22.7 (–<u>C</u>H$_2$–); 27.4–27.3 (–<u>C</u>H$_2$–CH=CH–), 25.8 (HC=CH–<u>C</u>H$_2$–CH=CH), 24.8 (–<u>C</u>H$_2$), 14.3, 14.2 (–<u>C</u>H$_3$).

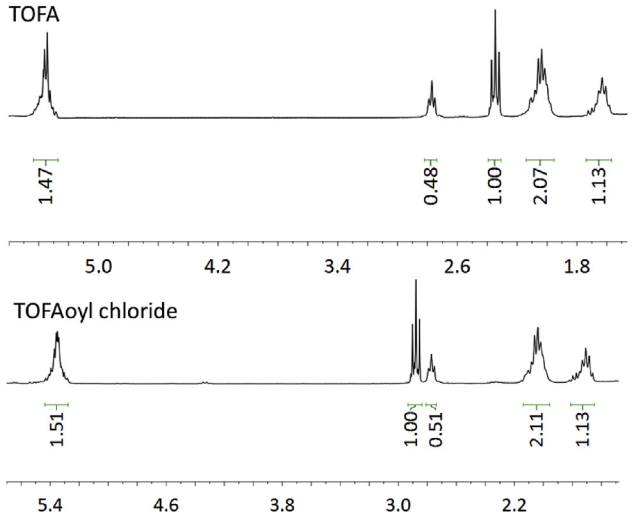

Figure A.1. Stacked ^{1}H NMR spectra of TOFA and TOFAoyl chloride (numbers below each peak represent the peak integration value).

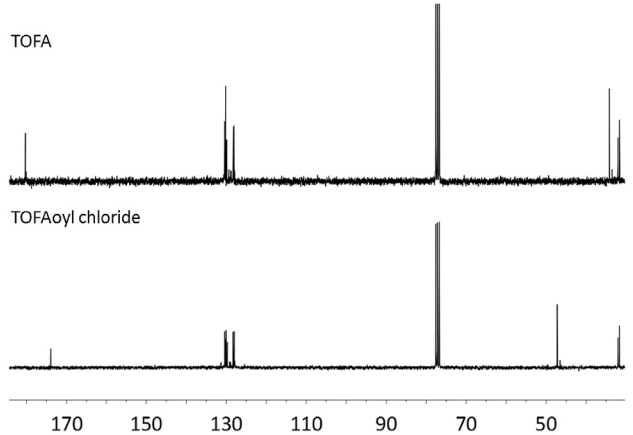

Figure A.2. Stacked ^{13}C NMR spectra of TOFA and TOFAoyl chloride.

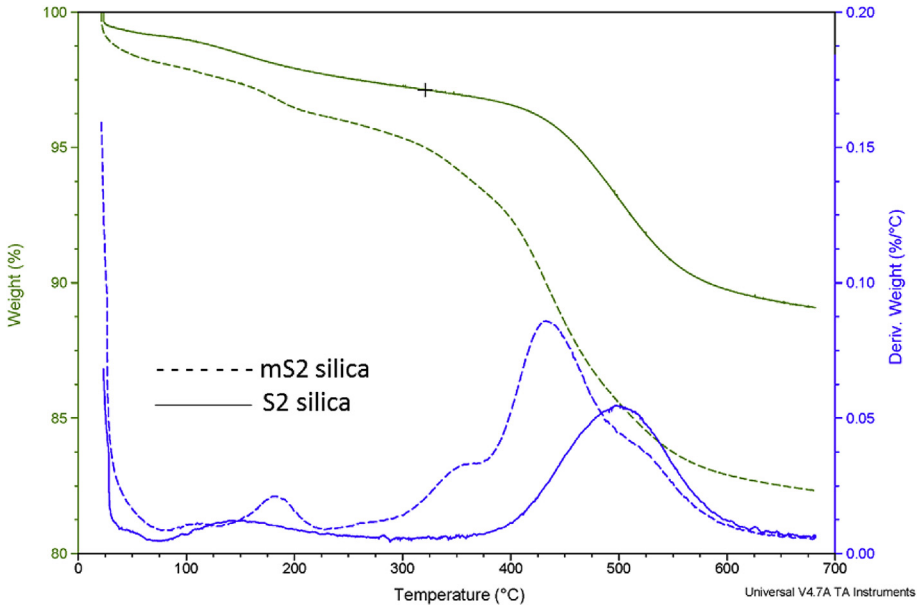

Figure A.3. Thermal gravimetric analysis (TGA) graph of the original silica (S2 – full line) and TOFA modified silica (mS2 – dash line); remaining weight percent of the sample versus temperature (green line) and derivative weight versus temperature (blue line) are shown.

Table A.1. Weight loss of the original silica (S2) and TOFA modified silica (mS2) in each arbitrary step during the TGA.

Sample	Weight loss in step 1[a] (%)	Weight loss in step 2[b] (%)	Final remaining weight (%)
S2	1.58	8.26	89.29
mS2	2.19	13.43	82.51

[a] Step 1 was measured from 75 °C to 250 °C (approximately).
[b] Step 2 was measured from 250 °C to 650 °C (approximately).

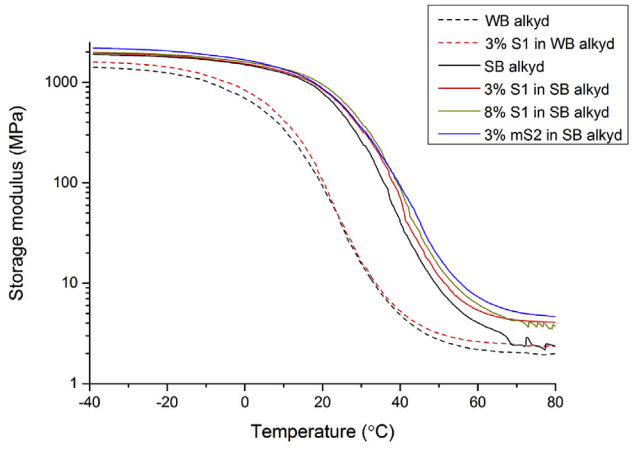

Figure A.4. Logarithmic scale of storage modulus as a function of temperature for pure alkyd and all the nano composites.

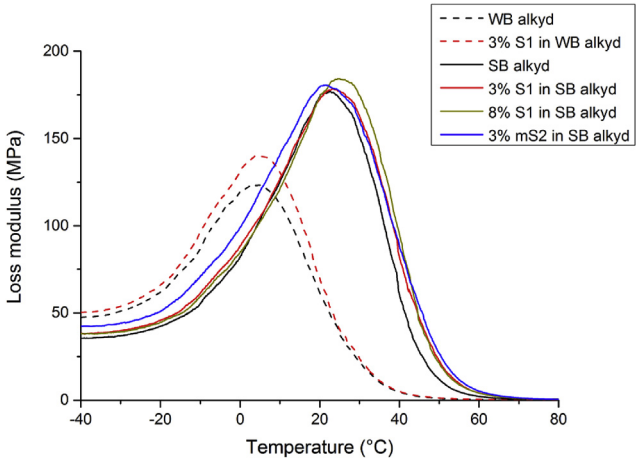

Figure A.5. Loss modulus as a function of temperature for pure alkyd and all the nano composites.

References

[1] M. Nikolic, J.M. Lawther, A.R. Sanadi, Use of nanofillers in wood coatings: a scientific review, J. Coat. Technol. Res. 12 (2015) 445–461.
[2] R. Wool, X.S. Sun, Nanoclay biocomposites, in: Bio-based Polymers and Composites, Academic Press, 2005, p. 641.
[3] P. Bordes, E. Pollet, L. Averous, Nano-biocomposites: Biodegradable polyester/nanoclay systems, Prog. Polym. Sci. 34 (2009) 125–155.
[4] S.R. Williams, Wood Handbook, Chapter 16: Finishing of Wood, Forest Products Laboratory, Forest Products Laboratory, Madison, WI: U.S, 2010.
[5] A.E. Boerman, D.Y. Perera, Measurement of stress in multicoat systems, J. Coat. Technol. 70 (1998) 69–75.
[6] D.Y. Perera, Physical ageing of organic coatings, Prog. Org. Coat. 47 (2003) 61–76.
[7] D.Y. Perera, On adhesion and stress in organic coatings, Prog. Org. Coat. 28 (1996) 21–23.
[8] O. Negele, W. Funke, Internal stress and wet adhesion of organic coatings, Prog. Org. Coat. 28 (1996) 285–289.
[9] A. Saadat-Monfared, M. Mohseni, Polyurethane nanocomposite films containing nano-cerium oxide as UV absorber; Part 2: Structural and mechanical studies upon UV exposure, Colloids Surf. A Physicochem. Eng. Asp. 441 (2014) 752–757.
[10] F. Aloui, A. Ahajji, Y. Irmouli, B. George, B. Charrier, A. Merlin, Photostabilisation of the "wood-clearcoatings" systems with UV absorbers: correlation with their effect on the glass transition temperature, J. Phys. Conf. Ser. 40 (2006) 118–123.
[11] F. Aloui, A. Ahajji, Y. Irmouli, B. George, B. Charrier, A. Merlin, Inorganic UV absorbers for the photostabilisation of wood-clearcoating systems: Comparison with organic UV absorbers, Appl. Surf. Sci. 253 (2007) 3737–3745.
[12] F. Bauer, R. Mehnert, UV Curable Acrylate Nanocomposites: Properties and Applications, J. Polym. Res. 12 (2005) 483–491.
[13] R. Rodriguez, S. Vargas, E. Rubio, S. Pacheco, M. Estevez, Abrasion Properties Of Alkyd- And Acrylic-Based Polymer-Ceramic Nano-Hybrid Coatings On Wood Surfaces, Mater. Res. Innov. 10 (2006) 193–206.
[14] M.M. Jalili, S. Moradian, H. Dastmalchian, A. Karbasi, Investigating the variations in properties of 2-pack polyurethane clear coat through separate incorporation of hydrophilic and hydrophobic nano-silica, Prog. Org. Coat. 59 (2007) 81–87.
[15] B.S. Kim, S.H. Park, B.K. Kim, Nanosilica-reinforced UV-cured polyurethane dispersion, Colloid Polym. Sci. 284 (2006) 1067–1072.
[16] N. Domun, H. Hadavinia, T. Zhang, T. Sainsbury, G.H. Liaghat, S. Vahid, Improving the fracture toughness and the strength of epoxy using nanomaterials - a review of the current status, Nanoscale 7 (2015) 10294–10329.
[17] P. Deligny, N. Tuck, Alkyds and polyesters, in: P.K.T. Oldring (Ed.), Resins for Surface Coatings, vol. II, John Wiley and Sons, 2001.
[18] D.S.P. Collins, Woodcare (interior and exterior architectural coatings): market statistics and technology development, in: PRA's 9th International Woodcoatings Congress, PRA, Amsterdam, Amsterdam, 2014.
[19] R.A. Sailer, M.D. Soucek, Viscoelastic properties of alkyd ceramers, J. Appl. Polym. Sci. 73 (1999) 2017–2028.
[20] R.P. Chartoff, J.D. Menczel, S.H. Dillman, Dynamic mechanical analysis, in: J.D. Menczel, R.B. Prime (Eds.), Thermal Analysis of Polymers: Fundamentals and Applications, John Wiley and Sons Inc., 2009.
[21] P. Bartolomeo, M. Irigoyen, E. Aragon, M.A. Frizzi, F.X. Perrin, Dynamic mechanical analysis and Vickers micro hardness correlation for polymer coating UV ageing characterisation, Polym. Degrad. Stab. 72 (2001) 63–68.
[22] R. Lamy, E. Zunic, R. Steding, A. Aamodt, Preparation of stable slurries of spherically shaped silica for coatings, Prog. Org. Coat. 72 (2011) 96–101.
[23] P.A. Gerin, Y. Grohens, R. Schirrer, Y. Holl, Adhesion of latex films. Part IV. Dominating interfacial effect of the surfactant, J. Adhes. Sci. Technol. 13 (1999) 217–236.
[24] J. Ekstedt, Influence of coating system composition on moisture dynamic performance of coated wood, J. Coat. Technol. 75 (2003) 27–37.
[25] B.C. Smith, Infrared Spectral Interpretation: a Systematic Approach, CRC Press, Boca Raton, 1998.
[26] N. Vlachos, Y. Skopelitis, M. Psaroudaki, V. Konstantinidou, A. Chatzilazarou, E. Tegou, Applications of Fourier transform-infrared spectroscopy to edible oils, Anal. Chim. Acta 573–574 (2006) 459–465.
[27] C. Duce, V. Della Porta, M.R. Tine, A. Spepi, L. Ghezzi, M.P. Colombini, E. Bramanti, FTIR study of ageing of fast drying oil colour (FDOC) alkyd paint replicas, Spectrochim. Acta A Mol. Biomol. Spectrosc. 130 (2014) 214–221.
[28] F.X. Perrin, M. Irigoyen, E. Aragon, J.L. Vernet, Artificial aging of acrylurethane and alkyd paints: a micro-ATR spectroscopic study, Polym. Degrad. Stab. 70 (2000) 469–475.
[29] M. Lazzari, O. Chiantore, Drying and oxidative degradation of linseed oil, Polym. Degrad. Stab. 65 (1999) 303–313.
[30] R. Ploeger, D. Scalarone, O. Chiantore, The characterization of commercial artists' alkyd paints, J. Cult. Herit. 9 (2008) 412–419.
[31] G. Ellis, M. Claybourn, S.E. Richards, The application of fourier transform raman spectroscopy to the study of paint systems, Spectrochim. Acta Part A Mol. Spectrosc. 46 (1990) 227–241.
[32] L.S. Schadler, L.C. Brinson, W.G. Sawyer, Polymer nanocomposites: A small part of the story, Jom 59 (2007) 53–60.
[33] J. Jordan, K.I. Jacob, R. Tannenbaum, M.A. Sharaf, I. Jasiuk, Experimental trends in polymer nanocomposites—a review, Mater. Sci. Eng. A 393 (2005) 1–11.
[34] S. Zhang, M. Guo, Z. Chen, Q.H. Liu, X. Liu, Grafting photosensitive polyurethane onto colloidal silica for use in UV-curing polyurethane nanocomposites, Colloids Surf. A Physicochem. Eng. Asp.s 443 (2014) 525–534.
[35] Y. Zamani Ketek Lahijania, M. Mohseni, S. Bastani, Characterization of mechanical behavior of UV cured urethane acrylate nanocomposite films loaded with silane treated nanosilica by the aid of nanoindentation and nanoscratch experiments, Tribol. Int. 69 (2014) 10–18.
[36] W.J. Muizebelt, J.C. Hubert, R.A.M. Venderbosch, Mechanistic study of drying of alkyd resins using ethyl linoleate as a model substance, Prog. Org. Coat. 24 (1994) 263–279.
[37] M.D. Soucek, T. Khattab, J. Wu, Review of autoxidation and driers, Prog. Org. Coat. 73 (2012) 435–454.
[38] M. Irigoyen, P. Bartolomeo, F.X. Perrin, E. Aragon, J.L. Vernet, UV ageing characterisation of organic anticorrosion coatings by dynamic mechanical analysis, Vickers microhardness, and infra-red analysis, Polym. Degrad. Stab. 74 (2001) 59–67.
[39] J.-J. Max, C. Chapados, Infrared spectroscopy of aqueous carboxylic acids: comparison between different acids and their salts, J. Phys. Chem. A 108 (2004) 3324–3337.
[40] G. Poulenat, S. Sentenac, Z. Mouloungui, Fourier-transform infrared spectra of fatty acid salts—Kinetics of high-oleic sunflower oil saponification, J. Surf. Deterg. 6 (2003) 305–310.
[41] F.X. Perrin, C. Merlatti, E. Aragon, A. Margaillan, Degradation study of polymer coating: Improvement in coating weatherability testing and coating failure prediction, Prog. Org. Coat. 64 (2009) 466–473.
[42] A.-C. Hellgren, P. Weissenborn, K. Holmberg, Surfactants in water-borne paints, Prog. Org. Coat. 35 (1999) 79–87.
[43] M. Ghaemy, S. Bekhradnia, Thermal and photocuring of an acrylate-based coating resin reinforced with nanosilica particles, J. Coat. Technol. Res. 9 (2012) 569–578.
[44] M. Ghaemy, S.M.A. Nasab, M. Barghamadi, Nonisothermal cure kinetics of diglycidylether of bisphenol-A/amine system reinforced with nanosilica particles, J. Appl. Polym. Sci. 104 (2007) 3855–3863.
[45] M.M. Jalili, S. Moradian, Deterministic performance parameters for an automotive polyurethane clearcoat loaded with hydrophilic or hydrophobic nanosilica, Prog. Org. Coat. 66 (2009) 359–366.
[46] L.R.G. Treloar, The Physics of Rubber Elasticity, third ed, Clarendon Press: Oxford University Press, Oxford New York, 2005.
[47] M. Nikolic, S. Barsberg, F.H. Larsen, D. Löf, K. Mortensen, A.R. Sanadi, Mechanical characteristics of alkyd binder reinforced by surface modified colloidal nano silica, Prog. Org. Coat. 90 (2016) 147–153.
[48] R.F. Boyer, Dependence of mechanical properties on molecular motion in polymers, Polym. Eng. Sci. 8 (1968) 161–185.
[49] S.V. Glass, S.L. Zelinka, Wood Handbook, Chapter 4: Moisture Relations and Physical Properties of Wood, Forest Products Laboratory, Madison, WI: U.S., 2010.